ChemPubSoc Europe

DOI: 10.1002/cctc.201700004

CHEMCATCHEM Full Papers

Edge-hydroxylated Boron Nitride for Oxidative Dehydrogenation of Propane to Propylene

Lei Shi,[a] Dongqi Wang,[b] Wei Song,[a] Dan Shao,[a] Wei-Ping Zhang,[a] and An-Hui Lu*[a]

Oxidative dehydrogenation of propane to olefins is a promising alternative route to industrialized direct dehydrogenation, but encounters the difficulty in selectivity control for olefins because of the overoxidation reactions that produce a substantial amount of undesired CO_2. Here we report edge-hydroxylated boron nitride, a metal-free catalyst, that efficiently catalyzed dehydrogenation of propane to propylene with superior selectivity (80.2%) but with only negligible CO_2 formation (0.5%) at a given propane conversion of 20.6%. Remarkable stability was evidenced by the operation of a 300 h test with steady conversion and product selectivity. The active BNO$^{\bullet}$ site, generated dynamically through hydrogen abstraction of B–OH groups by molecular oxygen, triggered propane dehydrogenation by selectively breaking the C–H bond but simultaneously shut off the pathway of propylene overoxidation towards CO_2.

Introduction

Propylene, which is one of the most important light olefins in the petrochemical industry, is currently produced mainly by catalytic cracking of petroleum-derived hydrocarbons or multistage coal-based methanol-to-olefins processes, both involving extensive energy consumption and significant emission of CO_2.[1] Direct catalytic dehydrogenation of propane to propylene has been developed as a more economical and environmentally friendly route and has been commercialized by UOP and ABB Lummus in the 1990s, using Pt- and CrO_x-based catalysts, respectively.[2] However, this process practically suffered from thermodynamic limitations in further prompting the reaction efficiency and also rapid catalyst deactivation by coking and catalyst sintering that required a frequent regeneration of the catalysts under harsh conditions.[3]

Oxidative dehydrogenation (ODH) of propane, catalyzed by transition-metal oxides and alkaline-earth metal oxychlorides,[4] offers an attractive alternative route with the prominent characters of free coking and no equilibrium limitation in propane conversion, but the selectivity toward propylene is often lower than in the direct dehydrogenation route, primarily because of overoxidation of the formed propylene to CO_2 (10–60%).[5] Under the reaction conditions, the formed electron-rich propylene reacted more easily with molecular oxygen over the metal oxide catalysts, resulting in the cleavage of the C–C bond through consecutive oxygen insertion and thus forming the final product, CO_2. From a chemical point of view, an ideal catalyst should be highly selective for C–H bond cleavage but not for C–C bond cleavage under the oxidative dehydrogenation conditions. Unfortunately, the development of such a highly selective catalyst is still challenging.

Recently, Hermans's group reported that boron nitride exhibits a high selectivity to propylene (79%) and ethylene (12%) at 14% conversion in the ODH reaction of propane.[6] Nevertheless, in view of activity, selectivity, and stability, there is still room for improvements, and a detailed structural characterization of this novel catalytic system and a better understanding of the structure–activity correlation in the ODH reaction of propane are still needed. As reported herein our group found that boron nitride, after steam hydroxylation at the edges, can efficiently catalyze the ODH of propane. We show that edge-hydroxylated boron nitride offers high selectivity toward propylene (up to 80.2%) at higher propane conversion (20.6%). At a 6.5% conversion level of propane, it offers a surprising propylene selectivity as high as 97.4%. As we aimed at understanding the catalytic origin of boron nitride in the ODH reaction of propane, we could show that the B–OH groups at the edges of boron nitride selectively activate the C–H bond in propane and simultaneously suppress the overoxidation of propylene into CO_2.

Results and Discussion

Oxidative dehydrogenation of propane

Boron nitride was first impregnated with 1 M sodium nitrite aqueous solution, followed by steam (5 vol.% H_2O/N_2) activation at 530 °C for 3 h; the resulting sample (BNOH) was washed with aqueous ammonia and finally calcined at 500 °C for 2 h in air. The BNOH catalyst provided surprisingly high selectivity toward propylene during ODH of propane at 530 °C. The conversion of

[a] Dr. L. Shi, W. Song, D. Shao, Prof. W.-P. Zhang, Prof. A.-H. Lu
State Key Laboratory of Fine Chemicals
School of Chemical Engineering
Dalian University of Technology
Dalian 116024 (China)
E-mail: anhuilu@dlut.edu.cn

[b] Prof. D. Wang
Center for Multi-Disciplinary Research
Institute of High Energy Physics
Chinese Academy of Sciences
Beijing 100049 (China)

Supporting information for this article can be found under: http://dx.doi.org/10.1002/cctc.201700004.

© 2017 Wiley-VCH Verlag GmbH & Co. KGaA, Weinheim

propane approached 20.6%, which is equivalent to a reaction rate of 7.74 $g_{C_3H_8}\ g_{cat}^{-1}\ h^{-1}$; the product slate consisted of propylene, ethylene, methane, CO, and CO_2. In particular, the selectivity was 80.2% for propylene and only 0.5% for CO_2 (Figure 1a). Taking the equally important product ethylene into account, the selectivity for light olefins (ethylene + propylene, $C_{2-3}^{=}$) was up to 90.9%, which was much higher than the selectivities obtained over the well-developed metal or metal oxide catalysts at a comparable propane conversion level, as well as over carbon and carbonaceous materials.[4b,5e,f,7] More significantly, the formation of CO_2 (0.5%) was considerably lower than for the traditional ODH processes (10–60% CO_2),[5] demonstrating the excellent performance of the current BNOH catalyst in the selective activation of the C–H bond in propane.

A control experiment with a feed gas of C_3H_6/O_2/He showed no measurable conversion of propylene (Supporting Information, Figure S1), evidencing that the BNOH catalyst does not activate the C–C bond of propylene and thus avoids its overoxidation under ODH conditions. The remarkable stability of the BNOH catalyst in the ODH of propane was evidenced by the operation of a 300 h test at 530 °C, in which no significant variations in the conversion and product selectivity occurred (Figure 1b), demonstrating the potential for industrial application. Moreover, the selectivity toward propylene can be further promoted by mediating the reaction conditions. For example, propylene selectivity of 97.4% ($C_{2-3}^{=}$: 99.1%) was obtained at 510 °C at a propane conversion level of 6.5%; whereas it approached 59.8% ($C_{2-3}^{=}$: 76.3%) at 540 °C with a propane conversion level of 38.2% (Figure S2).

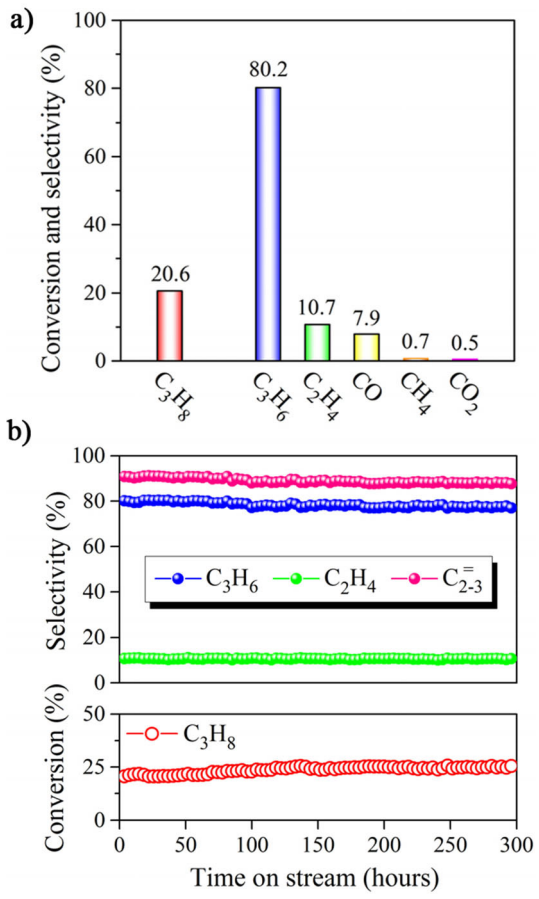

Figure 1. Oxidative dehydrogenation of propane over the BNOH catalyst. a) Propane conversion and product selectivity, b) long-term stability test. Reaction conditions: temperature, 530 °C; catalyst weight, 100 mg; gas feed, 16.7 vol.% C_3H_8, 25.1 vol% O_2, and He balance; space velocity, 37.6 $g_{C_3H_8}\ g_{cat}^{-1}\ h^{-1}$.

Structural characterization of the BNOH catalyst

To verify the origin of the unique selectivity of the BNOH catalyst, detailed structural analyses were conducted. The BNOH catalyst inherited a hexagonal layered structure of boron nitride (Figure S3). Aberration-corrected transmission electron microscopy (TEM) analyses identified the in-plane lattice retained its hexagonal symmetry with a large number of edges that were newly created during steam activation (Figure 2a, Figures S4 and S5). TEM images viewed along the [0 0 1] direction (Figure 2a and Figure S6) revealed that the most frequently exposed lateral termination facets were $\{1\,0\,\bar{1}\,0\}$, $\{0\,1\,\bar{1}\,0\}$, and $\{1\,\bar{1}\,0\,0\}$, suggesting that the terminated configuration had zigzag edges.[8] Lattice relaxations and distortions occurred exclusively at the edge of the layer (Figure 2a and Figure S7).

Boron K-edge electron energy-loss spectroscopy (EELS) analysis with a high-angle annular dark-field (HAADF) STEM mode (Figure 2b and Figure S8) showed that the edge possesses a higher π^* to σ^* ratio (1.27, point 2) than that (0.52, point 4) of the in-plane, primarily because of the local warp or wrinkle at the edge,[9] and the B/N ratio (1.28, point 2) at the edge was higher than that (0.95, point 4) of the in-plane (Figure 2b). X-ray photoelectron spectroscopy (XPS) analysis identified that the surface concentrations of boron and oxygen were 44.3% and 9.2% (Figure 2c), respectively. There were two types of boron species (Figure 2c); one was coordinated with nitrogen on the flat surface whereas the other was bonded to oxygen at the edge.[10] The chemical environment for the coordination between boron and oxygen was further verified by the 2D ^{11}B multiple quantum (MQ) magic-angle spinning (MAS) NMR spectrum of the BNOH catalyst (Figure 2d). There were two types of boron–oxygen bonding at 26.0 and 24.4 ppm; the former represents the edge boron sites bonded to two bridging oxygen atoms, and the latter corresponded to B–OH bonding, which was identified by the sharp ^1H resonance at 1.2 ppm in the ^1H MAS NMR spectrum (Figure 2d, inset).

Identification of active sites of the BNOH catalyst

FTIR analysis was performed to identify the roles of the B–O–B and B–OH groups under the reaction conditions. The characteristic band of hydroxyl stretching vibration was clearly observed at approximately 3400 cm^{-1} (Figure 3a).[11] Upon exposure to C_3H_8 atmosphere at 530 °C, the band position of the hydroxyl stretches remained unchanged, and no propane conversion was detected (Figure 3a). With the addition of molecular oxygen (O_2/C_3H_8/He), however, the absorption of hydroxyl vibrational stretches gradually weakened (Figure 3a), accompanied with the formation of propylene, indicating that the OH groups interacted with molecular oxygen and incorpo-

© 2017 Wiley-VCH Verlag GmbH & Co. KGaA, Weinheim
These are not the final page numbers!

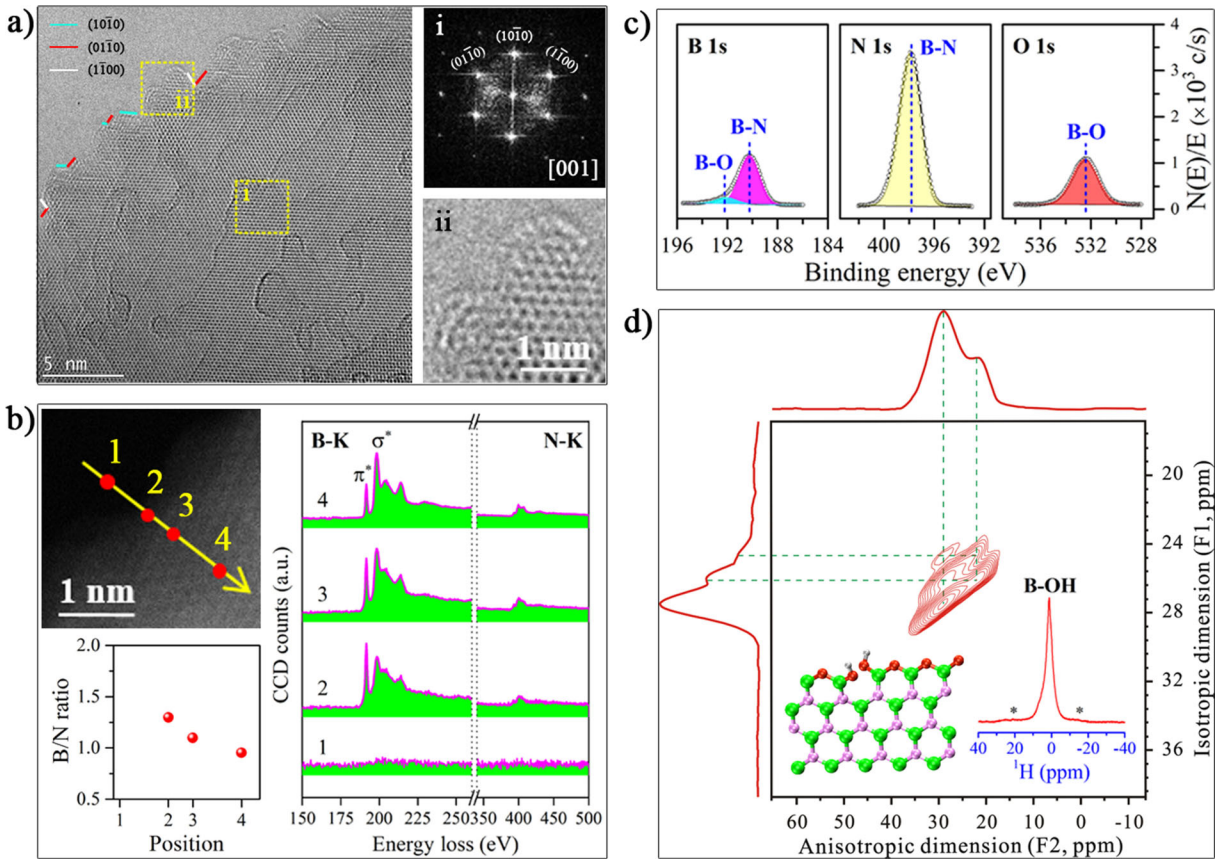

Figure 2. Structural characterization of the BNOH catalyst. a) Aberration-corrected TEM images along [0 0 1] direction and FFT image of the (i) and (ii) areas. b) HAADF–STEM image (top left), boron and nitrogen K-edge EELS spectrum (right), and B/N ratio (bottom left) calculated by the EELS spectrum. c) B 1s, N 1s, and O 1s XPS spectra. d) 2D ^{11}B MQ MAS NMR and ^{1}H MAS NMR (inset) spectra as well as the structural model (inset) of the BNOH edges.

rated into the reaction network. The intensities of hydroxyl vibrational stretches were fully recovered upon steam activation (Figure 3a and Figure S9), suggesting that the OH groups could be readily regenerated.

Isotopic measurements further confirmed the catalytic role of the B–OH groups. If C_3H_8 and O_2 were pulsed into the deuterated BNOH(D) catalyst at 530 °C, both HDO and D_2O were formed immediately, and their amounts gradually decreased during subsequent pulses (Figure 3b and Figure S10). This indicated that the H/D atoms in the BNOH(D) catalyst were abstracted during the reaction process. The neighboring oxygen atoms were also involved in the reaction process. If the BNOH catalyst was exposed to a mixture of $^{18}O_2$ and C_3H_8 (Figure 3c), both $H_2{}^{16}O$ and $H_2{}^{18}O$ were produced, suggesting that the ^{16}O atom in the B–OH groups participated in the formation of the $H_2{}^{16}O$ molecule. During subsequent pulses, the amount of $H_2{}^{18}O$ continuously increased while the amount of $H_2{}^{16}O$ decreased, further verifying the isotopic exchange between ^{16}O sites at the BNOH edge and gaseous $^{18}O_2$.

DFT calculations demonstrated that two adjacent B–OH groups could dehydrate through the transition state with a four-membered ring, leading to the formation of B–O–B bridges. Reversibly, the gaseous H_2O could insert into the B–O–B bridges to recover the two adjacent B–OH groups. The freshly formed $H_2{}^{18}O$ during the ODH will participate in the reversible breakage of the B–O–B bridges, through which the exchange between the gaseous ^{18}O and the ^{16}O at the BNOH edge site will be fulfilled, and the edge B–OH sites can remain at their active state (Figure S11).

Kinetic behavior of propane ODH over the BNOH catalyst

The kinetic characters of the ODH reaction of propane over the BNOH catalyst nicely supported the conclusion from in situ FTIR and isotope-labeling experiments. Initially, the apparent activation energies (E_a) of two reactants, propane and oxygen, were obtained by evaluating the dependence of their converting rates on the reaction temperature. It was found that the E_a of propane conversion was 184 kJ mol^{-1}, lower than that (≈250 kJ mol^{-1}) reported by Hermans's group.[6] In the current study, the E_a (213 kJ mol^{-1}) of oxygen activation was estimated to be higher than that of propane conversion (Figure 4a). This means that the cleavage of C–H bonds readily happens after oxygen activation in the BNOH catalytic system for the ODH of propane.

This deduction was further verified by measuring the kinetic isotope effects (KIEs) of C–H cleavage. The low KIEs for primary hydrogen abstraction ($k_{1,C-H}/k_{1,C-D}=1.4$ using C_3H_8 and $CH_3CD_2CH_3$ as reactants) and secondary hydrogen abstraction ($k_{2,C-H}/k_{2,C-D}=1.5$ using $CH_3CD_2CH_3$ and C_3D_8 as reactants) also indicated that the cleavage of C–H bonds readily happened in our BNOH catalytic system for propane ODH (Figure 4b), supporting the deduction from activation energy measurements.

© 2017 Wiley-VCH Verlag GmbH & Co. KGaA, Weinheim

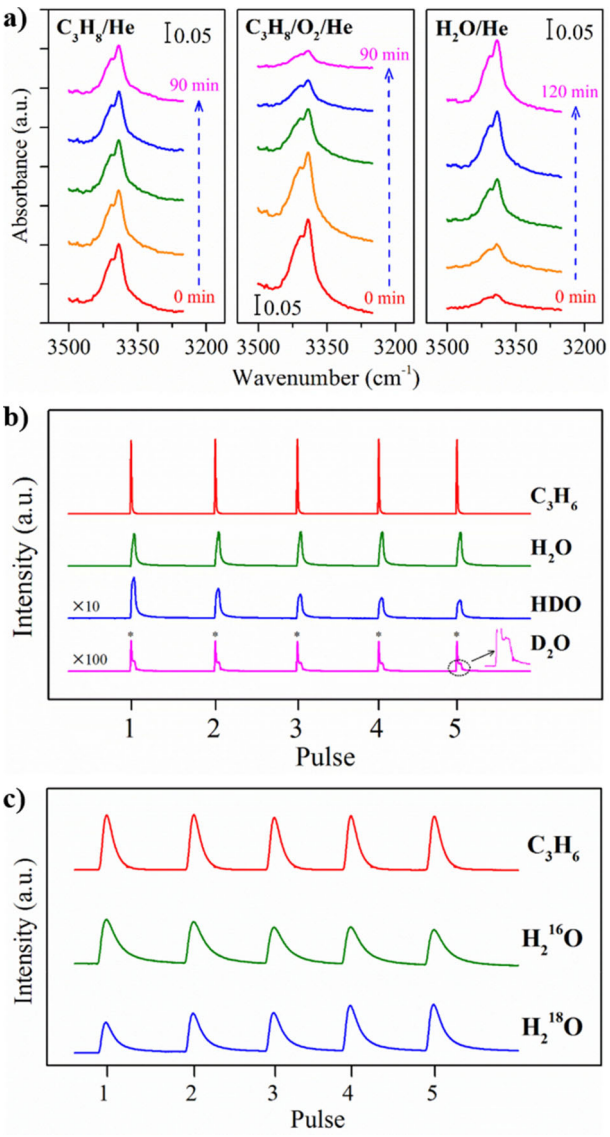

Figure 3. Identification of active sites of BNOH catalyst. a) FTIR spectra of the B–OH vibration over the BNOH catalyst under C_3H_8, C_3H_8/O_2/He, and H_2O/He atmospheres at 530 °C. b) Mass spectra of C_3H_6, H_2O, HDO, and D_2O species upon pulsing C_3H_8 and O_2 onto the deuterated BNOH(D) catalyst at 530 °C. c) Mass spectra of C_3H_6, $H_2{}^{16}O$ and $H_2{}^{18}O$ species during pulsing C_3H_8 and $^{18}O_2$ onto the BNOH catalyst at 530 °C.

Moreover, the effect of reactant concentrations on the reaction rate was measured to investigate the kinetic behaviors (Figure 4c and Figure 4d). A Langmuir-type dependence on oxygen concentration corresponds with a reaction mechanism that is controlled by adsorption or activation of molecular oxygen on the catalyst surface. Second-order dependence on propane concentration suggested that the propane reacted directly from the gas phase with the active oxygen species on the surface of the BNOH catalyst.[12]

Conclusions

We have demonstrated that boron nitride, upon steam activation to generate B–OH groups at the edges, efficiently catalyzes the oxidative dehydrogenation of propane with a superior selectivity toward propylene and a significantly minimized CO_2 emission. Hydrogen abstraction of B–OH groups by molecular oxygen dynamically generates the active sites, which triggers propane dehydrogenation. This novel and metal-free catalyst system not only opens up a new research direction in the selective activation of the C–H bond of alkanes, but also serves as a highly potential catalyst for the industrial ODH process.

Experimental Section

Catalyst preparation

Pristine boron nitride was synthesized by using a high-temperature solid-phase reaction employing boric acid (H_3BO_3) and melamine ($C_3H_6N_6$) together with urea ($CO(NH_2)_2$) as the boron and nitrogen sources, respectively. The typical synthesis procedure was as follows: H_3BO_3 (1.856 g) and $C_3H_6N_6$ (0.755 g) were dissolved in methanol (10 mL), and then $CO(NH_2)_2$ (0.269 g) was added into the solution. Subsequently, the methanol was completely evaporated at 25 °C under vigorous stirring conditions. The resulting solid was heated to 1500 °C and maintained at that temperature for 1 h in a graphite boat (total length, 55 mm; width, 22 mm; height, 22 mm) in a quartz-tube furnace under N_2 flow of 80 mL min^{-1}. The product was washed by using deionized water of 90 °C for three times and filtered to remove excess boron oxide. The white boron nitride had a specific surface area of 32 m^2 g^{-1} and a pore volume of 0.23 cm^3 g^{-1}.

The as-prepared boron nitride was hydroxylated by a sodium-assisted high-temperature steam activation process.[13] A typical procedure was as follows: sodium nitrite solution (200 μL, 1 mol L^{-1}) was initially impregnated in boron nitride powder (1.0 g) and then maintained at 50 °C for 6 h, followed by calcination in air at 560 °C for 1 h. After air cooling to room temperature, the solid product was transferred to a fixed-bed reactor and then treated with 5 vol.% H_2O/N_2 at 530 °C for 3 h. Sodium ions were further leached out at reflux in 3 mol L^{-1} ammonia at 80 °C for 3 times, followed by extensive washing with ultrapure water (40 times, 50 mL water each). The obtained powders were treated in air at 500 °C for 2 h with a heating rate of 10 °C min^{-1}, and the resultant sample was denoted as BNOH. The inductively coupled plasma optical emission spectroscopy (ICP–OES) measurement showed that the residual content of sodium was 0.18 wt.%.

Catalytic evaluation

Catalytic reactions were performed in a packed-bed quartz microreactor (I.D. = 6 mm). Prior to testing, the catalyst was heated to 560 °C at a rate of 10 °C min^{-1} in 20 vol.% O_2/N_2 and maintained at this temperature for 1 h. The reaction mixture was C_3H_8/O_2/He with a molar ratio of 1/1.5/3.5 at atmospheric pressure. The flow rate was fixed at 192 mL min^{-1}, and the reaction temperature was varied in the range of 500–550 °C. Reactants and products were analyzed by an online gas chromatograph (Techcomp, GC 7900). A GDX-102 and 5A molecular sieve column, connected to a TCD were used to analyze the O_2, He, C_3H_8, C_3H_6, C_2H_4, CH_4, CO, and CO_2.

Conversion was defined as the number of moles of carbon converted divided by the number of moles of carbon present in the feed. Selectivity was defined as the number of moles of carbon in the product divided by the number of moles of carbon reacted. The carbon balance was checked by comparing the number of

© 2017 Wiley-VCH Verlag GmbH & Co. KGaA, Weinheim

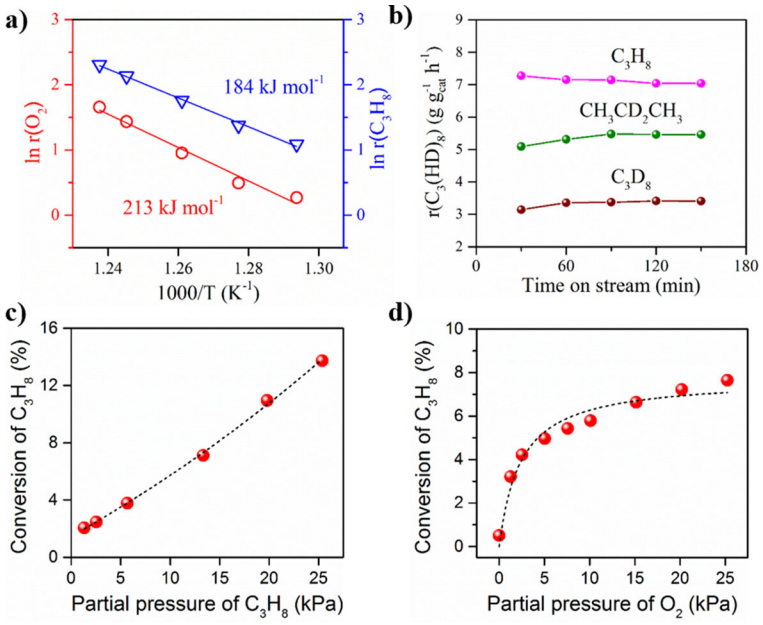

Figure 4. Kinetic behaviors of propane ODH over the BNOH catalyst. a) Arrhenius plots for the reaction rate (activation energy, E_a) of C_3H_8 (triangle symbols) and O_2 (circle symbols). Reaction rates of propane and oxygen were measured in the range of 500–535 °C with a feed gas of 16.7 vol% C_3H_8/25.1 vol% O_2/He at the space velocity of 75.2 $g_{C3H8}\,g_{cat}^{-1}\,h^{-1}$. b) Reaction rates of C_3H_8, $CH_3CD_2CH_3$, and C_3D_8 as function of reaction time in ODH of propane. Reaction rates were measured at 530 °C with a feed gas of 16.7 vol% C_3H_8 or $CH_3CD_2CH_3$ or C_3D_8/25.1 vol%O_2/He at the space velocity of 75.2 $g_{C3H8}\,g_{cat}^{-1}\,h^{-1}$. c) and d) Effect of partial pressure of propane and oxygen on propane conversion in the ODH reaction over the BNOH catalyst. Reaction conditions: catalyst weight, 100 mg; gas feed, 0–25.2 vol % C_3H_8, 0–25.2 vol% O_2, and He balance; reaction temperature, 530 °C; space velocity, 75.2 $g_{C3H8}\,g_{cat}^{-1}\,h^{-1}$; 0.1 MPa.

moles of carbon in the outlet stream to the number of moles of carbon in the feed. Under our typical evaluating conditions, the carbon balance was within ±3%. To account for the volume expansion in the reaction, helium was used as the internal standard.

In kinetic analysis, reaction rates were measured in a packed-bed single-pass flow microreactor with plug-flow hydrodynamics. Experimental data of propane and oxygen conversion at different temperature levels were used to obtain the apparent activation energy. Reaction orders of propane and oxygen were obtained by measuring the effect of reactant partial pressure on reaction rates. Catalytic reaction was supposed to proceed under net kinetic control.

Catalyst characterization

Powder X-ray diffraction (PXRD) measurements were performed on a Rigaku D/Max 2400 diffractometer using $Cu_{K\alpha}$ radiation (λ = 0.15406 nm). The powder catalyst was placed inside a quartz-glass sample holder prior to testing. Rietveld refinements of PXRD pattern were conducted with GSAS program.

HRTEM images were recorded on an aberration-corrected and monochromated FEI Titan ETEM 80–300 microscope. The microscope was operated at an accelerating voltage of 80 kV to limit structural damage to the sample. HAADF–STEM images and EELS were taken on an aberration-corrected Nion Ultra STEM 100 at 100 kV equipped with a Gatan Enfinium Spectrometer. The specimen was prepared by ultrasonically dispersing the powder sample in ethanol and droplets of the suspension were deposited onto a carbon-coated copper grid.

Solid-state MAS NMR spectra were recorded on an Agilent DD2-500 MHz spectrometer. ^{11}B and ^{1}H MAS NMR experiments were performed at 160.3 MHz and 499.8 MHz, respectively, using a 4-mm MAS NMR probe with a spinning rate of 10 kHz. ^{1}H MAS NMR spectra were accumulated for 32 scans with a 5 s recycle delay. The chemical shifts were referenced to tetramethylsilane (TMS). 2D ^{11}B multiple-quantum (MQ) MAS NMR experiments were performed using a three-pulse sequence incorporating a *z*-filter at a spinning speed of 10 kHz. A two-dimensional Fourier transformation followed by a shearing transformation gave a pure absorption mode 2D contour plot. The chemical shifts were referenced to a 1 M H_3BO_3 aqueous solution at 19.6 ppm. Prior to testing, the sample was dehydrated at 400 °C for 1 h at 10^{-4} Pa and then transferred to a 4-mm MAS rotor in a home-made device without exposure to air.

XPS analysis was performed on an Omicron Sphera II hemispherical electron energy analyzer with an in situ reaction cell attached to the instrument. Monochromatic AL K X-ray source (1486.6 eV, anode operating at 15 kV and 300 W) was used as incident radiation. The binding energy of the element was calibrated using an N 1s photoelectron peak at 398.1 eV.[10,14] Before the measurements, all the samples were treated in situ at 500 °C for 1 h under an Ar stream (32 mL min^{-1}) and then moved to the measured chamber under vacuum conditions.

ICP–OES measurements were conducted to monitor the sodium content in the hydroxylation process. The samples were dissolved in a mixture of HNO_3 and HF under microwave-assisted heating conditions. Nitrogen adsorption–desorption isotherms were measured with a Micromeritics TriStar 3000 adsorption analyzer. Before the measurements, the sample was degassed at 200 °C for 4 h. The specific surface area was calculated from the adsorption data in the relative pressure range from 0.05 to 0.3 using the BET method.

In situ infrared spectroscopy

In situ FTIR spectra were recorded under reaction condition on a Nicolet 6700 FTIR spectrometer equipped with mercury cadmium telluride (MCT) detector. The BNOH catalyst of ≈25 mg was compressed as a thin disk (Φ = 1.2 cm), and placed in a quartz transmission cell equipped with CaF_2 windows and a thermocouple mount that allowed direct measurement of the surface temperature. Spectra were averaged over 512 scans in the range 400–4000 cm^{-1} with a 2 cm^{-1} resolution. Prior to collecting spectra, the catalysts were pretreated for 1 h at 530 °C in helium (40 mL min^{-1}). The gas composition at the reactor outlet during in situ FTIR experiments was controlled by online mass spectrometry (MS, Pfeiffer, OminStar™). The propane and oxygen conversions were calculated from the inlet and outlet concentration of these components. The following mass-to-charge (*m*/*z*) signals were analyzed: 29 (C_3H_8), 32 (O_2), 41 (C_3H_6, C_3H_8), 44 (C_3H_8, CO_2), and 18 (H_2O). A rehydroxylation of the used catalysts was made with a 4 vol.% H_2O/He stream.

© 2017 Wiley-VCH Verlag GmbH & Co. KGaA, Weinheim

Isotope-labeling experiments

Isotopic tracer experiments were performed in a packed-bed single-pass flow microreactor. The chemical and isotopic compositions of the reactor effluent were measured by online mass spectrometry (MS, Pfeiffer, OminStar™) at 10 s intervals. In the deuterium-labeling studies, the BNOH catalyst was initially treated at 530 °C under helium (40 mL min^{-1}) for 1 h, and then a 6 h H/D exchange process on the BNOH surface was accomplished by passing a He feed (28 mL min^{-1}) through a water saturator held at 25 °C by a thermostat to produce a 3.5 vol.% D_2O/He feed. Heavy water (D_2O, Cambridge Isotope Lab., 99.9%) was not further purified. Subsequently, the deuterated BNOH catalyst was purged with the dry helium (32 mL min^{-1}) for 3 h to remove the excess D_2O. C_3H_8, O_2, or a mixture of the two (800 μL each time) was then directly pulsed into the deuterated BNOH catalyst using helium (32 mL min^{-1}) as the carrier gas. The products were analyzed by a mass spectrometer with the following mass-to-charge (*m/z*) signals: 29 for C_3H_8, 41 for C_3H_6, 32 for O_2, 18 for H_2O, 19 for HDO, and 20 for D_2O.

Before the ^{18}O-labeling experiments, the BNOH catalyst was treated at 530 °C under helium (40 mL min^{-1}) for 1 h and then the mixture of C_3H_8 and $^{18}O_2$ (800 μL each time) was pulsed into the BNOH catalyst using helium (40 mL min^{-1}) as the carrier gas. The products were analyzed by a mass spectrometer with the following *m/z* signals: 29 for C_3H_8, 41 for C_3H_6 and C_3H_8, 36 for $^{18}O_2$, 18 for $H_2{}^{16}O$, and 20 $H_2{}^{18}O$. Propane (C_3H_8, research grade, 99.99%), oxygen ($^{16}O_2$, research grade, 99.99%), and isotopic oxygen ($^{18}O_2$, Cambridge Isotope Lab., ≥99%) were used as reactants without further purification.

DFT calculations

All stationary points were fully optimized using the B3LYP hybrid exchange–correlation functional[15] as implemented in Gaussian 09 program with all atoms described by a double ξ quality basis set, 6-31G(d, p),[16] followed by vibrational frequency analysis to identify the stationary points, either as minima or transition states. Intrinsic reaction coordinate (IRC) calculations[17] were performed to confirm that each transition state connects the two minima along the reaction pathway.

Acknowledgements

We thank Dr. Yan Zhou (Dalian Institute of Chemical Physics, Chinese Academy of Sciences) for assistance on TEM measurements, Prof. Mingshu Chen (Xiamen University, China) for his assistance on XPS measurements, and Prof. Wenjie Shen (Dalian Institute of Chemical Physics, Chinese Academy of Sciences) for the valuable discussions. This work was financially supported by National Natural Science Foundation of China (21225312, U1462120, 21473206, and 21373035) and Cheung Kong Scholars Program of China (T2015036). A Chinese patent and an international patent application under the Patent Cooperation Treaty are pending.

Conflict of interest

The authors declare no conflict of interest.

Keywords: boron · dehydrogenation · hydrocarbons · hydroxylation · nitrides

[1] a) A. Corma, F. V. Melo, L. Sauvanaud, F. Ortega, *Catal. Today* **2005**, *107*, 699–706; b) J. Z. Li, Y. X. Wei, J. R. Chen, P. Tian, X. Su, S. R. Xu, Y. Qi, Q. Y. Wang, Y. Zhou, Y. L. He, Z. M. Liu, *J. Am. Chem. Soc.* **2012**, *134*, 836–839; c) L. S. Zhong, F. Yu, Y. L. An, Y. H. Zhao, Y. H. Sun, Z. J. Li, T. J. Lin, Y. J. Lin, X. Z. Qi, Y. Y. Dai, L. Gu, J. S. Hu, S. F. Jin, Q. Shen, H. Wang, *Nature* **2016**, *538*, 84–87.

[2] a) J. J. H. B. Sattler, J. Ruiz-Martinez, E. Santillan-Jimenez, B. M. Weckhuysen, *Chem. Rev.* **2014**, *114*, 10613–10653; b) J. C. Bricker, *Top. Catal.* **2012**, *55*, 1309–1314.

[3] a) K. J. Caspary, H. Gehrke, M. Heinritz-Adrian, M. Schwefer, *Handbook of Heterogeneous Catalysis*, Vol. 6 (Eds.: G. Ertl, H. Knozinger, F. Schüth, J. Weitkamp), Wiley-VCH, Germany, **2008**, pp. 3206–3229; b) L. Shi, G.-M. Deng, W.-C. Li, S. Miao, Q.-N. Wang, W.-P. Zhang, A.-H. Lu, *Angew. Chem. Int. Ed.* **2015**, *54*, 13994–13998; *Angew. Chem.* **2015**, *127*, 14200–14204.

[4] a) E. McFarland, *Science* **2012**, *338*, 340–342; b) F. Cavani, N. Ballarini, A. Cericola, *Catal. Today* **2007**, *127*, 113–131; c) C. A. Carrero, R. Schlögl, I. E. Wachs, R. Schomaecker, *ACS Catal.* **2014**, *4*, 3357–3380.

[5] a) L. Leveles, K. Seshan, J. A. Lercher, L. Lefferts, *J. Catal.* **2003**, *218*, 296–306; b) S. R. G. Carrazán, C. Peres, J. P. Bernard, M. Ruwet, P. Ruiz, B. Delmon, *J. Catal.* **1996**, *158*, 452–476; c) Y. M. Liu, Y. Cao, N. Yi, W. L. Feng, W. L. Dai, S. R. Yan, H. Y. He, K. N. Fan, *J. Catal.* **2004**, *224*, 417–428; d) R. B. Watson, U. S. Ozkan, *J. Catal.* **2000**, *191*, 12–29; e) S. Vajda, M. J. Pellin, J. P. Greeley, C. L. Marshall, L. A. Curtiss, G. A. Ballentine, J. W. Elam, S. Catillon-Mucherie, P. C. Redfern, F. Mehmood, P. Zapol, *Nat. Mater.* **2009**, *8*, 213–216; f) Q. H. Zhang, C. J. Cao, T. Xu, M. Sun, J. Z. Zhang, Y. Wang, H. L. Wan, *Chem. Commun.* **2009**, 2376–2378; g) M. A. De León, C. D. L. Santos, L. Latrónica, A. M. Cesio, C. Volzone, J. Castiglioni, M. Sergio, *Chem. Eng. J.* **2014**, *241*, 336–343.

[6] J. T. Grant, C. A. Carrero, F. Goeltl, J. Venegas, P. Mueller, S. P. Burt, S. E. Specht, W. P. McDermott, A. Chieregato, I. Hermans, *Science* **2016**, *354*, 1570–1573.

[7] W. Qi, D. S. Su, *ACS Catal.* **2014**, *4*, 3212–3218.

[8] L. Bourgeois, Y. Bando, T. Sato, *J. Phys. D* **2000**, *33*, 1902–1908.

[9] N. Alem, Q. M. Ramasse, C. R. Seabourne, O. V. Yazyev, K. Erickson, M. C. Sarahan, C. Kisielowski, A. J. Scott, S. G. Louie, A. Zettl, *Phys. Rev. Lett.* **2012**, *109*, 205502.

[10] K. H. Lee, H.-J. Shin, B. Kumar, H. S. Kim, J. Lee, R. Bhatia, S.-H. Kim, I.-Y. Lee, H. S. Lee, G.-H. Kim, J.-B. Yoo, J.-Y. Choi, S.-W. Kim, *Angew. Chem. Int. Ed.* **2014**, *53*, 11493–11497; *Angew. Chem.* **2014**, *126*, 11677–11681.

[11] a) A. Bhattacharya, S. Bhattacharya, G. P. Das, *Phys. Rev. B* **2012**, *85*, 035415; b) T. Sainsbury, A. Satti, P. May, Z. M. Wang, I. McGovern, Y. K. Gun'ko, J. Coleman, *J. Am. Chem. Soc.* **2012**, *134*, 18758–18771.

[12] R. Grabowski, *Catal. Rev. Sci. Eng.* **2006**, *48*, 199–268.

[13] a) X. L. Li, X. P. Hao, M. W. Zhao, Y. Z. Wu, J. X. Yang, Y. P. Tian, G. D. Qian, *Adv. Mater.* **2013**, *25*, 2200–2204; b) F. Xiao, S. Naficy, G. Casillas, M. H. Khan, T. Katkus, L. Jiang, H. K. Liu, H. J. Li, Z. G. Huang, *Adv. Mater.* **2015**, *27*, 7196–7203; c) Q. H. Weng, X. B. Wang, X. Wang, Y. Bando, D. Golberg, *Chem. Soc. Rev.* **2016**, *45*, 3989–4012.

[14] A. Pakdel, Y. Bando, D. Golberg, *ACS Nano* **2014**, *8*, 10631–10639.

[15] a) A. D. Becke, *Phys. Rev. A* **1988**, *38*, 3098–4100; b) C. T. Lee, W. T. Yang, R. G. Parr, *Phys. Rev. B* **1988**, *37*, 785–789; c) B. Miehlich, A. Savin, H. Stoll, H. Preuss, *Chem. Phys. Lett.* **1989**, *157*, 200–206.

[16] V. A. Rassolov, J. A. Pople, M. A. Ratner, T. L. Windus, *J. Chem. Phys.* **1998**, *109*, 1223–1229.

[17] a) H. P. Hratchian, H. B. Schlegel, *J. Chem. Phys.* **2004**, *120*, 9918–9924; b) H. P. Hratchian, H. B. Schlegel, *J. Chem. Theory Comput.* **2005**, *1*, 61–69; c) H. P. Hratchian, H. B. Schlegel in *Theory and Applications of Computational Chemistry* (Eds.: C. E. Dykstra, G. Frenking, K. S. Kim, G. Scuseria), Elsevier, Amsterdam, **2005**, pp. 195–249.

Manuscript received: January 2, 2017
Revised: January 24, 2017
Accepted Article published: January 31, 2017
Final Article published: ■■ ▮▮, 0000

© 2017 Wiley-VCH Verlag GmbH & Co. KGaA, Weinheim

Olefin generation without a metal: Edge-hydroxylated boron nitride shows superior selectivity for the oxidative dehydrogenation of propane to propylene with only negligible CO_2 formation. The dynamically generated active BNO$^{\bullet}$ site triggers propane dehydrogenation by selectively breaking the C–H bond by concomitantly avoiding propylene oxidation to CO_2.

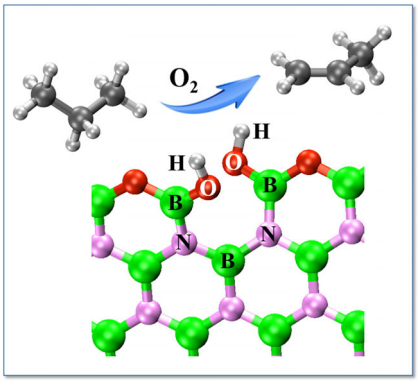

*L. Shi, D. Wang, W. Song, D. Shao, W.-P. Zhang, A.-H. Lu**

■■ – ■■

Edge-hydroxylated Boron Nitride for Oxidative Dehydrogenation of Propane to Propylene

© 2017 Wiley-VCH Verlag GmbH & Co. KGaA, Weinheim

These are not the final page numbers! ↗↗